CONDITIONING RESERVOIR MODELS TO WELL TEST INFORMATION

CLAYTON V. DEUTSCH
Stanford Center for Reservoir Forecasting, Stanford, CA, USA, 94305

Pressure transient well test information has largely been ignored in stochastic reservoir modeling. Well testing informs the effective absolute permeability of some region around the well. This information does not resolve local details of the spatial distribution of permeability; however, it does constrain the average permeability. This paper presents an approach, based on simulated annealing, that will condition stochastic reservoir models to such well test-derived effective properties.

The volume and type of averaging informed by the well test must first be calibrated by forward simulating the well test on stochastic reservoir models that are consistent with the geological interpretation, core data, well log data, and seismic data. Stochastic reservoir models are then constructed with simulated annealing where one component of the global objective function relates to honoring the well test-derived average permeability.

INTRODUCTION

The concept underlying stochastic reservoir modeling is to construct numerical models of the reservoir properties that are consistent with all relevant data. Applying a flow simulator to multiple numerical models allows an appreciation for the uncertainty in the reservoir response. The accuracy and precision of the output response distribution requires integrating a maximum amount of relevant prior information, e.g., core plug measurements, well log data, surface and borehole geophysical interpretations, geological interpretations, spatial information gathered from similar reservoirs, properties inferred from well tests, ... This paper is concerned with integrating this last source of data, i.e., effective permeabilities inferred from pressure transient well tests, into stochastic models of absolute permeability.

Conventional conditional simulation techniques such as Gaussian [6,18], fractal [10], or indicator [13] models have the ability to account for local conditioning data (core and well log data), a global histogram, and varying amounts of spatial information in the form of two-point variogram/covariance models. Variants of these techniques based on cokriging [7] or some type of trend model [17] allow geophysical information to be integrated into the resulting realizations. However, none of these techniques allow the integration of well test-derived effective permeabilities.

Simulation techniques based on marked point processes [9] are well-suited to simulating spatial phenomenon that are characterized by a repetition of easily character-

ized shapes. The resulting spatial structure is implicitly controlled by the placement of the digitized or analytical shapes. Conditioning to local data and a global histogram is achieved by disallowing inconsistencies at data locations and controlling the number of objects placed in the realization. The integration of geophysical interpretations and well test-derived effective permeabilities is not possible with these latter techniques.

A well test-derived effective permeability does not directly inform the smaller scale permeability values near the well bore. However, it does constrain a complex non-linear average of the small scale values. Many flow processes are directly influenced by the average flow characteristics as informed by well test-derived effective permeabilities. Historically, well test-derived permeabilities were used in homogeneous reservoir models for reservoir performance forecasting [20]. Two inadequacies of such homogeneous models are that they do not allow an assessment of uncertainty and they do not allow for the important influence of small scale permeability heterogeneities. Stochastic reservoir models allow the small scale permeability heterogeneities to be accounted for. However, as mentioned above, current stochastic modeling techniques do not account for the information carried by average properties measured by well tests.

The problem of conditioning stochastic models to well test-derived effective permeability is difficult because the average is non-linear. Conventional simulation techniques allow data of different volumetric supports only when the averaging is linear, see page 513 [14].

One way to achieve this conditioning would be to discard all models that do not yield a forward simulated well test response close enough to the actual measured pressure response. Such selection procedures may be practical when building models with a single well test; however, it is not practical in presence of multiple well test interpretations, some with more advanced multirate tests which inform a number of different permeability averages near the well. In general, a prohibitively large number of realizations would be required to find a few that simultaneously match all well test data.

The algorithm proposed in this paper is to generate realizations with *simulated annealing* [15] that honor the measured well test effective permeabilities in addition to conventional data such as the local conditioning data, a histogram, and a variogram/covariance. Application of simulated annealing requires that the generation of a stochastic realization be posed as an optimization problem. The two-part objective function in this optimization problem consists of the deviation from the desired statistical/geological description plus the deviation from the well test effective permeabilities. The deviation from the measured well test results could be known through forward simulation of the well test on all candidate realizations. Again, it would be impractical to forward simulate the well test after each (set of) perturbation(s) as demanded by simulated annealing. Therefore, the forward simulation must be replaced by a more easily calculated numerical approximation. A non-linear power average [3,5,16] of the small scale permeability values has been adopted for this purpose.

More precisely, the well test is first interpreted to provide the effective permeability near the well bore. Second, the type of averaging, as quantified by an averaging power, and the volume of averaging must be calibrated. The averaging power depends essentially on the connectivity of the extreme permeability values. The volume of averaging depends on the duration of the well test. Third, the initial stochastic realizations are altered by systematically changing the elementary grid block per-

meability values so that the previously calculated effective permeability and the variogram model are honored. Calculation of that effective permeability can be done very fast after each (set of) perturbation(s) using the previously calibrated power average.

The following presentation of the algorithm will clarify the implementation details and acknowledge a number of limitations. One limitation is that the method imposes the well test results without accounting for uncertainty in the underlying well test interpretation. A second limitation is that the method requires that the full well test response be summarized by a single non-linear weighted power average. The severity of these limitations may be judged through numerical experimentation.

QUANTIFYING WELL TEST-DERIVFED EFFECTIVE PERMEABILITY

Pressure transient well tests are performed by generating some flow rate impulse in the reservoir (e.g., start production, change the flow rate, stop production, ...) and measuring the pressure response. Well test interpretation consists of interpreting the pressure response by using some appropriate mathematical model to relate the pressure response (output) to flow rate history (input) [11]. Provided that the mathematical model is appropriate the model parameters can be associated to certain reservoir parameters. Of particular interest is the effective absolute permeability k_e.

To apply the envisaged optimization technique it is necessary to translate this well test effective k_e into a more easily calculated property while retaining the flexibility to differentiate a wide variety of heterogeneous systems encountered in practice. The power averaging formalism is used to model the non-linear averaging of absolute permeabilities [5]. The assumption is that the elementary permeability values average linearly after a non-linear power transformation, i.e.,

$$\overline{k}(\omega) = \left[\frac{1}{N} \sum_{\mathbf{u}_i \in V} k(\mathbf{u}_i)^{\omega} \right]^{\frac{1}{\omega}} \tag{1}$$

Where $\overline{k}(\omega)$ is the ω-power average permeability of the N permeability values $k(\mathbf{u}_i)$, $i = 1, \ldots, N$, at locations $\mathbf{u}_i$ within the volume of interest V. The power ω varies between the bounding values of -1 and 1 corresponding to the harmonic and arithmetic averages respectively (the geometric average is obtained for ω=0.0). The idea is to use relation (1) and to calibrate the averaging volume V and averaging power ω for each particular reservoir.

To define the appropriate averaging volume it is necessary to consider the portion of the pressure response used to derive the well test effective permeability k_e. In practice, k_e is obtained by interpreting the pressure response during the time at which the response resembles infinite-acting radial flow. Early-time effects such as wellbore storage and late-time boundary effects are not considered in the interpretation. It is possible to define an inner radius r_{min} and an outer radius r_{max} that correspond to the limits of infinite acting radial flow since the pressure response, at any time t, may be related to block permeabilities within a time-dependent radius-of-drainage $r(t)$. Consider a typical pressure response shown on the Miller-Dyes-Hutchinson (MDH) plot at the bottom of Figure 1. The pressure response between 1 hour and 10 hours is used to derive an estimate of the effective permeability $k_{welltest}$. The inner and outer limits of the shaded region (on the schematic illustration of the reservoir) correspond to the radius-of-drainage at 1 hour and 10 hours respectively.

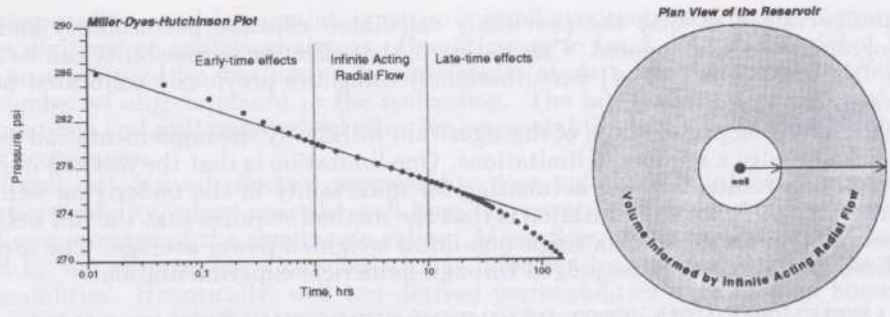

Figure 1: A schematic illustration of the volume measured by a given well test interpretation. The inner and outer limits of the shaded region, on the schematic illustration of the reservoir, correspond to the radius-of-drainage at 1 hour and 10 hours (the limits of infinite acting radial flow).

The time interval during which the pressure response resembles infinite-acting radial flow is easily determined by standard interpretation techniques. Evaluating the radius-of-drainage $r(t)$ at the time limits is not as straightforward; depending on the arbitrary definition chosen for $r(t)$, the radius can change by as much as a factor of 4. It will be necessary to calibrate the radius-of-drainage $r(t)$ by repeated flow simulations. The block permeabilities contributing to the pressure response measured up to time t are approximately enclosed by a circular volume centered at the well defined by a time-dependent radius $r(t)$ written as [3,12,21]:

$$r(t) = A\sqrt{\frac{k_e t}{\phi \mu c_t}} \tag{2}$$

where A is a constant, k_e is the reservoir permeability around the well, ϕ is the porosity, μ is the fluid viscosity, and c_t is the total compressibility. Depending on the definition chosen for the radius-of-drainage the value of A varies from 0.023 to 0.07 (for oil field units). Alabert [3], in the context of evaluating the averaging volume of a well test, and for specified levels of discretization and test durations, found an optimal A_{opt} value of 0.010 in oil field units.

The averaging power ω describes the type of averaging within the volume $V(A)$. In many cases, this averaging power is close to the geometric average ($\omega = 0$). For practical test durations and for complex heterogeneous permeability distributions, the type of averaging can differ significantly from the geometric average.

The constant A and the averaging power ω are calibrated with the following procedure (see also [3,4]):

1. Generate n_s (20-100) multiple realizations of the permeability field with relevant statistical properties.

2. Forward simulate a well test, with conditions as close as possible to those used in the field to arrive at k_e, on each realization to obtain n_s pressure response curves.

3. Deduce an effective permeability $\overline{k}_i, i = 1, \ldots, n_s$ from each pressure curve using established well test interpretation techniques [11].

4. Compute average permeabilities $\overline{k}(A,\omega)_i, i = 1,\ldots,n_s$ for A values between the practical bounding limits of 0.001 and 0.020 and for ω values between practical bounding limits of -0.5 and 0.5.

5. Choose the pair (A_{opt},ω_{opt}) that yields the closest agreement between the reference $\overline{k}_i, i = 1,\ldots,n_s$ values and the approximate $\overline{k}(A_{opt},\omega_{opt})_i, i = 1,\ldots,n_s$ values.

After establishing appropriate A_{opt} and ω_{opt} values the *goodness* of the power average approximation can be checked by plotting a scatterplot of the $\overline{k}(A_{opt},\omega_{opt})_i$ values versus the well test-derived $\overline{k}_i$ values.

The weighted non-linear power average (1) is proposed as a computationally simple replacement for the full 3-D well-test response. In practice, a well test response is interpreted to yield an estimate of the effective permeability k_e and the averaging volume parameter A_{opt} and power ω_{opt} are calibrated for the particular geological setting. The next step is to impose the well test-derived effective permeability k_e, i.e., the appropriate ω-average $\overline{k}(A_{opt},\omega_{opt})$, on stochastic models. The technique of simulated annealing is considered for this simulation.

SIMULATED ANNEALING

In the "annealing" approach to stochastic simulation there is no explicit random function model, rather, the creation of a simulated realization is formulated as an optimization problem to be solved with a stochastic relaxation or "annealing" technique. The first requirement of this class of methods is an objective (or energy) function which is some measure of difference between the desired spatial characteristics and those of a candidate realization. The essential feature of annealing methods is to iteratively perturb (relax) the candidate realization and then accept or reject the perturbation with some decision rule. The decision rule is based on how much the perturbation has brought the candidate image closer to having the desired properties. One possible decision rule is based on an analogy with the metallurgical process of annealing, hence the name *simulated annealing*. Technically the name "simulated annealing" only applies to those stochastic relaxation methods based strictly on simulated annealing [2,15]; however, through common usage the name "annealing" is used to describe the entire family of methods that are based on the principle of stochastic relaxation.

Annealing is the process where a metallic alloy is heated, without leaving the solid phase, so that molecules may move positions relative to one another and reorder themselves into a low energy crystal (or grain) structure. The probability that any two molecules will move relative to one another is known to follow the Boltzmann distribution. Simulated annealing is the application of the annealing mechanism of perturbation (swap the attribute values assigned to two different grid node locations) with the Boltzmann probability distribution for accepting perturbations.

At first glance this approach appears terribly inefficient. For example, millions of perturbations may be required to arrive at an image that has the desired spatial structure. However, these methods are more efficient than they might seem as long as few arithmetic operations are required to update the objective function after a perturbation; virtually all conventional *global* spatial statistics (e.g., a covariance) may be updated locally rather than globally recalculated after a local perturbation. Also, the power average representation of the well test k_e developed earlier is easily updatable.

The objective function is defined as some measure of difference between a set of reference properties and the corresponding properties of a candidate realization. The reference properties could consist of any *quantified* geological, statistical, or engineering property. In the context of this paper the reference properties consist of traditional two-point variogram/covariance functions and the well test derived effective permeability. Thus the objective function could be written as:

$$O = \lambda_1 \cdot \sum_{i=1}^{i=n_{\mathbf{h}}} \left[C^{reference}(\mathbf{h}_i) - C^{realization}(\mathbf{h}_i) \right]^2 + \lambda_2 \cdot \sum_{j=1}^{j=n_K} \left[k_{e_j}^{reference} - k_{e_j}^{realization} \right]^2 \tag{3}$$

where O is the objective function, $n_{\mathbf{h}}$ is the number of covariance lags $\mathbf{h}_i$ considered important, $C^{reference}(\mathbf{h}_i)$ is the ith reference covariance value, $C^{realization}(\mathbf{h}_i)$ is the ith covariance value taken from the candidate realization, n_K is the number of well test-derived effective permeabilities to be reproduced, $k_{e_j}^{reference}$ is the jth well test-derived effective permeability, $k_{e_j}^{realization}$ is the jth effective permeability calculated from the candidate realization using power averages, and λ_1 and λ_2 are relative weights to ensure that the covariance contribution has the same importance as the well test contribution.

The starting image is a 3-D array, $z(\mathbf{u}_i), i = 1, \ldots, N$, or permeability values. The annealing methodology to achieve a realization l, $z^{(l)}(\mathbf{u}_i), i = 1, \ldots, N$, with a low objective function (3) is as follows:

1. Establish the reference components in the objective function: the reference covariance values $C^{reference}(\mathbf{h}_i), i = 1, \ldots, n_{\mathbf{h}}$ are based on experimental data or on an analytical model. The reference effective permeabilities $k_{e_j}^{reference}, j = 1, \ldots, n_K$, are the direct result of applying standard interpretation techniques to the pressure transient response measured in the field.

2. Generate an easily constructed initial realization: the initial realization is either the output of a more conventional stochastic simulation algorithm or the initial realization could be generated by assigning each nodal value at random from the stationary univariate distribution $F(z)$.

3. Compute the realization components in the objective function: the covariance values $C^{realization}(\mathbf{h}_i), i = 1, \ldots, n_{\mathbf{h}}$, and the effective permeabilities $k_{e_j}^{realization}$, $j = 1, \ldots, n_K$, are calculated from the candidate realization.

4. Compute the objective function O based on the reference and the realization statistics, see (3).

5. Perturb the realization $z(\mathbf{u}_i), i = 1, \ldots, N$, to generate a new realization $z_{new}(\mathbf{u}_i)$, $i = 1, \ldots, N$ by swapping the permeability value at any two locations $\mathbf{u}_i$, $\mathbf{u}_j$, $i \neq j$, $0 < i,j \leq N$.

6. Update each component in the objective function and recompute the objective function O_{new} with the perturbation. The change to the objective function is $\Delta O = O_{new} - O_{old}$.

7. The perturbation is accepted or rejected on the basis of a specified decision rule. One approach would be to accept all helpful perturbations $\Delta O \leq 0$ and to reject all disruptive perturbations $\Delta O > 0$. This choice, which corresponds to a steepest descent approach, can lead to a local minima. The essential contribution of simulated annealing is a prescription for when to accept or reject a given perturbation. The acceptance probability distribution is given by:

$$P\{accept\} = \begin{cases} 1, & \text{if } \Delta O \leq 0 \\ e^{\frac{-\Delta O}{t}}, & \text{otherwise} \end{cases} \tag{4}$$

All favorable perturbations ($\Delta O \leq 0$) are accepted and some unfavorable perturbations are accepted with an exponential probability distribution. The parameter t of the exponential distribution is analogous to the "temperature" in annealing. The higher the temperature the more likely an unfavorable perturbation will be accepted.

Accepting the perturbation causes the image, $z(\mathbf{u}_i), i = 1, \ldots, N$, and the objective function O to be updated.

8. When the objective function O gets close to zero then the realization is considered finished since it now honors both the reference covariance and the well test data; otherwise, return to step 5 and continue the perturbation process.

The idea is to start with an initially high temperature parameter t (say the initial objective function $t = O$) and lower it by some multiplicative factor λ (say 0.1) when enough perturbations have been accepted (K_{accept}=10 times the number of grid nodes in the system N) or too many have been tried ($K_{max} = 100 \cdot N$). The algorithm is stopped when efforts to lower the objective function become sufficiently discouraging [19].

One remaining issue is to establish the weights λ_1 and λ_2 applied to each component in the objective function. The purpose behind these weights is to have each component play an equally important role in the global objective function. Without any weighting the component with the largest units would dominate the objective function. The weights λ_1 and λ_2 are established so that, in average, each component contributes equally to a change in the objective function ΔO. That is, each weight λ_c is inversely proportional to the average change of that component objective function:

$$\lambda_c = \frac{1}{\overline{|\Delta O_c|}}, \quad c = 1, \ldots, 2 \tag{5}$$

In practice, the average change of each component $\overline{|\Delta O_c|}$ can not be computed analytically; however, it can be numerically approximated by evaluating the average change of M (say 1000) independent perturbations:

$$\overline{|\Delta O_c|} = \frac{1}{M} \sum_{m=1}^{M} |O_c^{(m)} - O_c|, \quad c = 1, \ldots, 2 \tag{6}$$

where $\overline{|\Delta O_c|}$ is the average change for component c, $O_c^{(m)}$ is the perturbed objective value, and O_c is the initial objective value. Each of the M perturbations $m = 1, \ldots, M$ arises from the swapping mechanism employed for the annealing simulation.

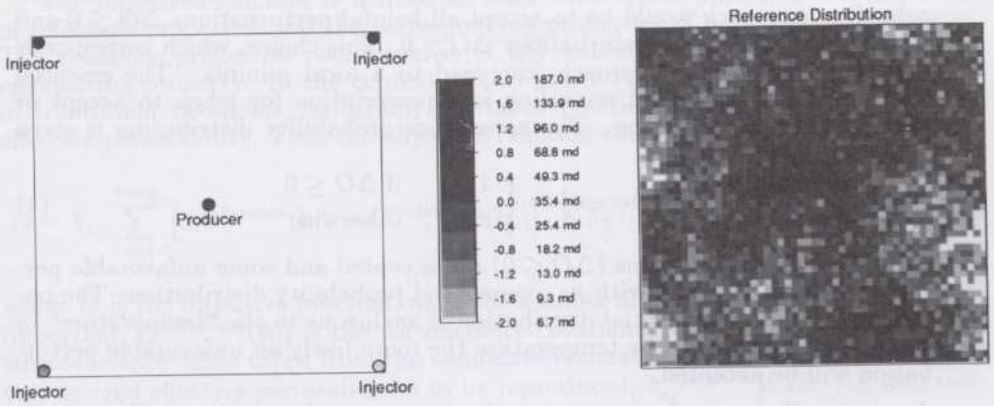

Figure 2: The reference distribution of permeability considered as the true reservoir for the purposes of obtaining the well test response and interpreted effective permeability.

All of the elements needed for integrating well test data are now in place. The resulting realizations obtained after going through the simulated annealing procedure with the objective function (3) are conditional to both the initial geological/statistical description and the well test-derived permeabilities. The following example illustrates how the methodology is implemented in practice.

AN EXAMPLE APPLICATION

Consider a 2-D example where the the block horizontal absolute permeabilities are known to follow a lognormal distribution $F(z)$ with a mean of 50.0 md and a variance of 2500 md^2. The distribution of log permeability is characterized by an exponential normal scores covariance model $C_Y(\mathbf{h})$ with an effective range of 25 grid block units. A 51 unit by 51 unit realization of this lognormal permeability field was generated to serve as a reference distribution, see Figure 2. The permeability at the central producer and the four injectors are known. Interpretation of a simulated drawdown response yields an estimated effective permeability of 102.1 md.

Simulated annealing is capable of generating realizations conditional to the distribution model $F(z)$, the covariance model $C_Y(\mathbf{h})$, and the five conditioning data. One hundred such realizations were generated by annealing with the objective function:

$$O = \sum_{i=1}^{i=n_{\mathbf{h}}} \left[C^{reference}(\mathbf{h}_i) - C^{realization}(\mathbf{h}_i) \right]^2$$

where $n_{\mathbf{h}}$ corresponds to the most compact arrangement of 18 lags, see top of Figure 3. Annealing allows this objective function to go to zero, i.e., the resulting realizations provide an excellent reproduction of the covariance. The first two realizations are shown on Figure 3.

These 100 initial realizations reproduce the measured permeability at the five well locations. However, a forward simulation of a well test at the producing well location does not yield the 102.1 md value obtained from the reference image. Figure 4 shows a histogram of the 100 permeability values. These 100 effective permeability values were used to calibrate the parameters A_{opt} and ω_{opt} that provide the best numerical approximation to the well test result. The average permeabil-

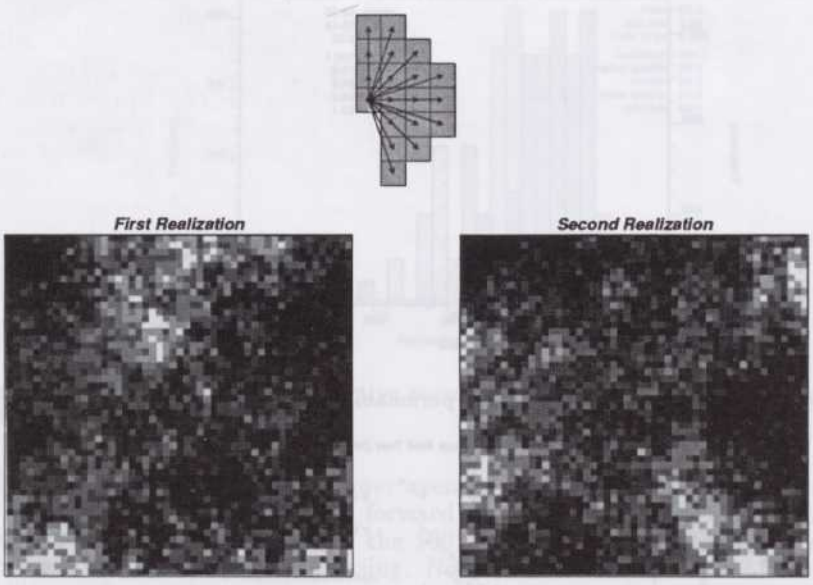

Figure 3: The lag vectors used to generate realizations of permeability and the first two realizations.

ities $\overline{k}(A,\omega)_i, i = 1,\ldots,n_s$ for A values between the practical bounding limits of 0.001 and 0.020 and for ω values between practical bounding limits of -0.5 and 0.5 were computed using the 100 initial realizations. The criteria for an optimal pair (A_{opt},ω_{opt}) was to minimize the mean normalized absolute deviation and the mean normalized error [3] defined as:

$$mNAD(A,\omega) = \sum_{i=1}^{i=n_s} \frac{|\overline{k}(A,\omega)_i - \overline{k}_i|}{\overline{k}_i} \tag{7}$$

$$mNE(A,\omega) = |\frac{\sum_{i=1}^{i=n_s} \overline{k}(A,\omega)_i - \sum_{i=1}^{i=n_s} \overline{k}_i}{\sum_{i=1}^{i=n_s} \overline{k}_i}| \tag{8}$$

$mNAD$ measures correlation and mNE measures the bias between the power average approximation and the true well test values. The optimal pair $A_{opt} = 0.003$ and $\omega_{opt} = 0.10$ was found to minimize both error terms.

Figure 5 shows a scatterplot of the power average numerical approximation and the true well test-derived effective permeability. Note the lack of any bias (the average effective permeabilities are 58.3 md in both cases) and the excellent correlation of 0.98. The physical volume informed by the well test can be determined by the constant A_{opt} and knowledge of the time limits of the infinite acting portion of the pressure response: $r_{min} = 1.0$ grid units (70.1 feet) and $r_{max} = 4.6$ grid units (320.0 feet).

The annealing simulation now uses a two part objective function (3). Annealing is able to generate realizations that lower this objective function to zero. The first two realizations are shown on Figure 6.

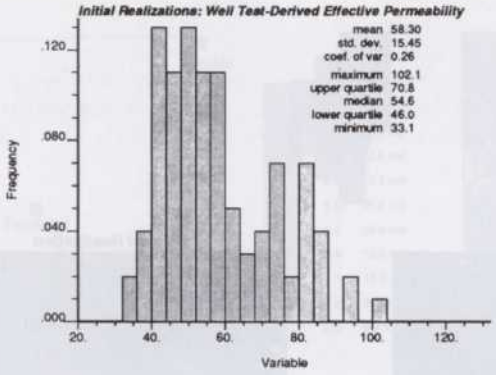

Figure 4: The histogram of 100 effective permeability values from the initial realizations.

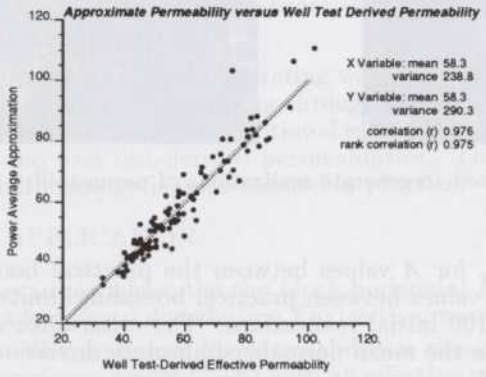

Figure 5: A scatterplot of the power average approximation and the true well test-derived effective permeabilities for all 100 initial realizations.

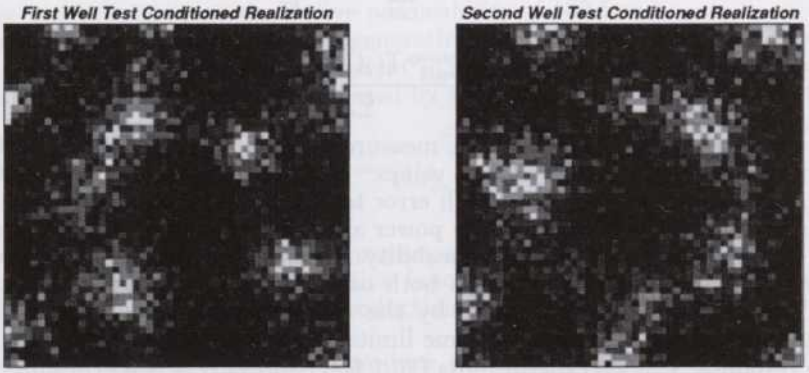

Figure 6: The first two realizations conditional to the five well data, the histogram, the covariance, and the well test result.

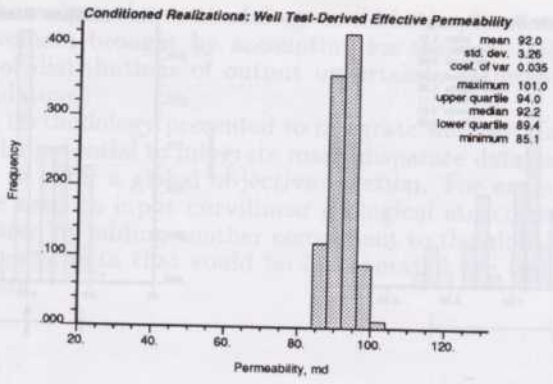

Figure 7: The histogram of 100 effective permeability values conditional to the well test result.

To verify that the calibrated power average is a fair approximation to the actual well test result a full well test was forward simulated on the final 100 realizations. Figure 7 shows the distribution of the 100 well test derived effective permeability values before and after post processing. Note that the distribution of effective permeabilities, after post processing, is much closer to the reference value of 102.2 md.

This illustrates that well test effective permeabilities can be imposed on stochastic realizations to a fair degree of approximation. What has not been shown is that accounting for well test-derived effective permeability actually helps predicting future reservoir performance. To illustrate the improvement in future prediction all 201 realizations (the reference, the 100 initial, and the 100 well test conditioned realizations) have been associated to the five spot injection/production pattern shown on the left of Figure 2 with an injector at all corner locations and a central producer. All variables except the block absolute permeabilities have been held constant and the performance of each realization has been simulated with Eclipse [1].

Two response variables are presented here: 1) the breakthrough time, i.e., the time of first water arrival at the producer, and 2) the final oil in place after 50 *years* of simulated production (note that the units are important only in a relative sense). The reference image yielded a breakthrough time of 0.81 time units and a fractional final oil in place 0.38. The histograms of values obtained before and after conditioning to the well test data on Figure 8. The results are summarized on Table 1. Note that the well test conditioned distributions are better centered around the reference value and the uncertainty as measured by the 95% probability interval $(q_{0.975} - q_{0.025})$ has been reduced.

REMARKS AND CONCLUSIONS

A methodology has been presented to integrate well test-derived properties into stochastic reservoir models. The methodology consists of generating realizations with simulated annealing. The objective is to minimize deviations from the initial variogram/covariance model and yet honor a numerical approximation of the well test-derived effective permeability. The power average numerical approximation is useful because it would not be feasible to re-run a flow simulation after each perturbation called for by the annealing technique.

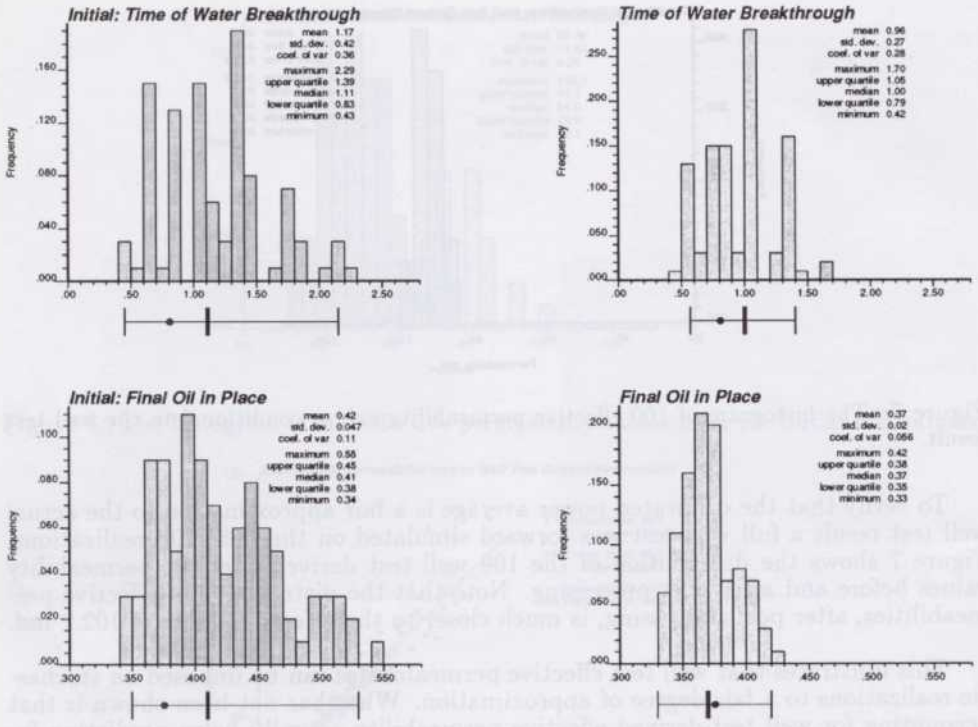

Figure 8: The histograms of the breakthrough time and the final oil in place obtained by running flow simulations on the realizations before (to the left) and after (to the right) integrating the well test data. The black dot in the lower box plot is the reference value, the thicker vertical line is the median, and the outermost vertical lines represent the 95% probability interval.

Response Variable		95% Probability Interval			percent
		$q_{0.025}$	$q_{0.5}$	$q_{0.975}$	reduction
Breakthrough time	reference		0.81		
	before	0.45	1.11	2.15	
	after	0.57	1.00	1.40	-51%
Final oil recovery	reference		0.38		
	before	0.35	0.41	0.53	
	after	0.33	0.37	0.42	-50%

Table 1: Summary of the breakthrough time and final water flow rate before and after conditioning to include the well test result. The reference values of 0.81 and 0.38 are shown under the median ($q_{0.5}$) column, the 95% probability intervals as established from the 100 flow simulations are shown by the 0.025 and 0.975 quantiles ($q_{0.025}$ and $q_{0.975}$), and the percent reduction refers to the width of the 95% probability interval.

An example shows how the methodology could be implemented in practice. The significant improvement brought by accounting for the well test data was demonstrated in terms of distributions of output uncertainty (after performing a water-flooding flow simulation).

The annealing methodology presented to integrate well test data is quite general. The method has the potential to integrate many disparate data as long as these data can be quantified to enter a global objective function. For example, multiple-point statistics could be used to input curvilinear geological structures and seismic data could be incorporated by adding another component to the global objective function [4,8]. Other sources of data that could be incorporated are the results of multiple rate and tracer tests.

References

[1] *ECLIPSE Reference Manual.* Exploration Consultants Limited, Highlands Farm, Greys Road, Henley-on-Thames, Oxon, England, November 1984.

[2] E. Aarts and J. Korst. *Simulated Annealing and Boltzmann Machines.* John Wiley & Sons, New York, NY, 1989.

[3] F. Alabert. Constraining description of randomly heterogeneous reservoirs to pressure test data: a Monte Carlo study. In *SPE Annual Conference and Exhibition, San Antonio*, Society of Petroleum Engineers, October 1989.

[4] C. Deutsch. *Annealing Techniques Applied to Reservoir Modeling and the Integration of Geological and Engineering (Well Test) Data.* PhD thesis, Stanford University, Stanford, CA, 1992.

[5] C. Deutsch. Calculating effective absolute permeability in sandstone/shale sequences. *SPE Formation Evaluation*, 343–348, September 1989.

[6] C. Deutsch and A. Journel. *GSLIB: Geostatistical Software Library.* to be published by Oxford University Press, New York, NY, 1992.

[7] P. Doyen. Porosity from seismic data: a geostatistical approach. *Geophysics*, 53(10):1263–1275, 1988.

[8] P. Doyen and T. Guidish. Seismic discrimination of lithology: a Bayesian approach. In *Geostatistics Symposium*, Calgary, AB, May 1990.

[9] H. Haldorsen and E. Damsleth. Stochastic modeling. *J. of Pet. Technology*, 404–412, April 1990.

[10] T. Hewett. Fractal distributions of reservoir heterogeneity and their influence on fluid transport. 1986. SPE paper # 15386.

[11] R. Horne. *Modern Well Test Analysis.* Petroway Inc, 926 Bautista Court, Palo Alto, CA, 94303, 1990.

[12] P. Johnson. The relationship between radius of drainage and cumulative production. *SPE Formation Evaluation*, 267–270, March 1988.

[13] A. Journel and F. Alabert. New method for reservoir mapping. *J. of Pet. Technology*, 212–218, February 1990.

[14] A. Journel and C. J. Huijbregts. *Mining Geostatistics*. Academic Press, New York, NY, 1978.

[15] S. Kirkpatrick, C. Gelatt Jr., and M. Vecchi. Optimization by simulated annealing. *Science*, 220(4598):671–680, May 1983.

[16] G. Korvin. Axiomatic characterization of the general mixture rule. *Geoexploration*, 19:267–276, 1981.

[17] A. Marechal. Kriging seismic data in presence of faults. In G. Verly et al., editors, *Geostatistics for natural resources characterization*, pages 271–294, Reidel, Dordrecht, Holland, 1984.

[18] G. Matheron, H. Beucher, H. de Fouquet, A. Galli, D. Guerillot, and C. Ravenne. Conditional simulation of the geometry of fluvio-deltaic reservoirs. 1987. SPE paper # 16753.

[19] W. Press, B. Flannery, S. Teukolsky, and W. Vetterling. *Numerical Recipes*. Cambridge University Press, New York, NY, 1986.

[20] H. Ramey Jr. Advances in practical well test analysis. In *65th Annual Technical Conference and Exhibition*, pages 665–676, Society of Petroleum Engineers, September 1990.

[21] H. van Poollen. A hard look at radius of drainage and stabilization-time equations. *Oil and Gas Journal*, 139–147, September 1964.